Hadronic vacuum polarization contributions to the muon g-2 in the space-like region

Elisa Balzani[a,b], Stefano Laporta[b,c], Massimo Passera[b]

[a] *Dipartimento di Fisica e Astronomia 'G. Galilei', Università di Padova, Italy*
[b] *Istituto Nazionale di Fisica Nucleare, Sezione di Padova, Padova, Italy*
[c] *Dipartimento di Fisica, Università di Bologna e Istituto Nazionale di Fisica Nucleare, Sezione di Bologna, Bologna, Italy*

Abstract

We present simple exact analytic expressions to compute the hadronic vacuum polarization contribution to the muon g-2 in the space-like region up to next-to-leading order. These results can be employed in lattice QCD calculations of this contribution, as well as in space-like determinations based on scattering data, like that expected of the proposed MUonE experiment at CERN.

1. Introduction

The Muon g-2 (E989) experiment at Fermilab has recently presented their first measurement of the muon magnetic moment anomaly, $a_\mu = (g-2)/2$ [1–4], confirming the earlier results of the E821 experiment at Brookhaven [5]. The E989 experiment is expected to reach a sensitivity four-times better than the E821 one. In addition, a new low-energy approach to measuring the muon g-2 is being developed by the E34 collaboration at J-PARC [6].

The present muon g-2 experimental average shows an intriguing 4.2σ discrepancy with the value for the Standard Model (SM) a_μ prediction quoted by the Muon g-2 Theory Initiative [7]. If confirmed with high significance, this discrepancy would be indirect evidence for new physics beyond the SM.

The main uncertainty of the muon g-2 SM prediction origins from its hadronic vacuum polarization (HVP) contribution, $a_\mu^{\rm HVP}$, which cannot be reliably calculated perturbatively in QCD and relies on experimental data as input to dispersion relations. Indeed, this contribution has been traditionally computed via a dispersive, or time-like, integral using hadronic production cross sections in low-energy electron-positron annihilation [8–13].

An alternative determination of $a_\mu^{\rm HVP}$ can be provided by lattice QCD. Significant progress has been made in the last few years in first-principles calculations of its leading order (LO) part, $a_\mu^{\rm HVP}$(LO), although these results are, in general, not yet competitive with the time-like determinations based on experimental data. Recently, the BMW collaboration presented the first lattice QCD determination of $a_\mu^{\rm HVP}$(LO) with an impressive sub-percent (0.8%) relative accuracy [14]. This remarkable result weakens the long-standing discrepancy between the SM muon g-2 prediction and the experimentally measured value. However, this result shows tension with the time-like data-driven determinations of $a_\mu^{\rm HVP}$(LO), being 2.2σ higher than the Muon g-2 Theory Initiative data-driven value. Moreover, shifts up of the $e^+e^- \to$ hadrons cross section, due to unforeseen missing contributions, to increase $a_\mu^{\rm HVP}$(LO) and solve the present muon g-2 discrepancy, lead to conflicts with the global electroweak fit if they occur at energies higher than ~ 1 GeV (and below that energy they are deemed improbable given the large required increases in the hadronic cross section) [15–19]. A new and competitive determination of the HVP contribution to the muon g-2, based on a method alternative to the time-like and lattice QCD ones, is therefore desirable.

A novel approach to determine the leading hadronic contribution to the muon g-2, measuring the effective electromagnetic coupling in the space-like region via scattering data, was proposed a few years ago [20]. The elastic scattering of high-energy muons on atomic electrons has been identified as an ideal process for this measurement, and a new experiment, MUonE, has been proposed at CERN to measure the shape of the differential cross section of muon-electron elastic scattering as a function of

the space-like squared momentum transfer [21–23].

In this paper we investigate the HVP contributions to the muon g-2 in the space-like region. At LO, simple results are long known and form the basis for the present lattice QCD and future MUonE determinations of $a_\mu^{\rm HVP}$(LO). Our goal is to provide simple exact analytic expressions to extend the space-like calculation of the $a_\mu^{\rm HVP}$ contribution to next-to-leading order (NLO).

2. The HVP contribution at leading order

2.1. Time-like method

Consider the hadronic component of the vacuum polarization tensor with four-momentum q,

$$i\Pi_{\rm h}^{\mu\nu}(q) = i\Pi_{\rm h}(q^2)\left(g^{\mu\nu}q^2 - q^\mu q^\nu\right) = \int {\rm d}^4x\; e^{iqx}\langle 0|T\left\{j_{\rm em}^\mu(x) j_{\rm em}^\nu(0)\right\}|0\rangle, \quad (1)$$

where $j_{\rm em}^\mu(x)$ is the electromagnetic hadronic current and $\Pi_{\rm h}(q^2)$ is the renormalized hadronic vacuum polarization function satisfying the condition $\Pi_{\rm h}(0) = 0$. The function $\Pi_{\rm h}(q^2)$ cannot be calculated in perturbation theory because of the non-perturbative nature of the strong interactions at low energy. Yet, the optical theorem ${\rm Im}\Pi_{\rm h}(s) = (\alpha/3)R(s)$, where the R-ratio is

$$R(s) = \frac{\sigma(e^+e^- \to \text{hadrons})}{4\pi\alpha^2/(3s)} \quad (2)$$

and α is the fine-structure constant, allows to express the imaginary part of the hadronic vacuum polarization in terms of the measured cross section of the process $e^+e^- \to$ hadrons as a function of the positive squared four-momentum transfer s. This result forms the basis for the time-like method.

The leading-order hadronic contribution to the muon g-2 can be calculated integrating experimental time-like (i.e. $q^2 > 0$) data using the well-known formula [24–26]

$$a_\mu^{\rm HVP}({\rm LO}) = \frac{\alpha}{\pi^2}\int_{s_0}^\infty \frac{{\rm d}s}{s}\, K^{(2)}(s/m^2)\, {\rm Im}\Pi_{\rm h}(s), \quad (3)$$

where m is the muon mass and $s_0 = m_{\pi^0}^2$. Defining

$$z = \frac{q^2}{m^2} \quad (4)$$

and the rationalizing variable

$$y(z) = \frac{\sqrt{z} - \sqrt{z-4}}{\sqrt{z} + \sqrt{z-4}}, \quad (5)$$

the second-order function $K^{(2)}(z)$ for $z \geq 0$ is

$$K^{(2)}(z) = \frac{1}{2} - z + \left(\frac{z^2}{2} - z\right)\ln z + \frac{\ln y(z)}{\sqrt{z(z-4)}}\left(z - 2z^2 + \frac{z^3}{2}\right). \quad (6)$$

For $z \geq 0$, $K^{(2)}(z)$ is real, positive and monotonic. At $z = 0$, $K^{(2)}(0) = 1/2$, while for $z \to +\infty$ the asymptotic behaviour of the kernel function is $K^{(2)}(z) \to 1/(3z)$, therefore vanishing at infinity.

2.2. Space-like method

The time-like expression for $a_\mu^{\rm HVP}$(LO) provided by Eq. (3) can be rewritten using the dispersion relation satisfied by $K^{(2)}(z)$ [27],

$$K^{(2)}(z) = \frac{1}{\pi}\int_{-\infty}^0 {\rm d}z'\, \frac{{\rm Im}K^{(2)}(z')}{z' - z}, \quad z > 0. \quad (7)$$

Indeed, replacing $K^{(2)}(s/m^2)$ in Eq. (3) with Eq. (7) and integrating over s via the subtracted dispersion relation satisfied by $\Pi_{\rm h}(q^2)$,

$$\frac{\Pi_{\rm h}(q^2)}{q^2} = \frac{1}{\pi}\int_{s_0}^\infty \frac{{\rm d}s}{s}\frac{{\rm Im}\Pi_{\rm h}(s)}{s - q^2}, \quad q^2 < 0, \quad (8)$$

we obtain the space-like expression

$$a_\mu^{\rm HVP}({\rm LO}) = -\frac{\alpha}{\pi^2}\int_{-\infty}^0 \frac{{\rm d}t}{t}\,\Pi_{\rm h}(t)\,{\rm Im}K^{(2)}(t/m^2). \quad (9)$$

The function $K^{(2)}(z)$, real for any $z \geq 0$, has a cut along the negative real axis $z < 0$ with the imaginary part

$${\rm Im}K^{(2)}(z + i\epsilon) = \pi\,\theta(-z)\left[\frac{z^2}{2} - z + \frac{z - 2z^2 + z^3/2}{\sqrt{z(z-4)}}\right] = \pi\,\theta(-z)\,F^{(2)}(y(z)), \quad (10)$$

where

$$F^{(2)}(y) = \frac{y+1}{y-1}\,y^2. \quad (11)$$

The $i\epsilon$ prescription, with $\epsilon > 0$, indicates that, in correspondence of the cut, the function ${\rm Im}K^{(2)}(z)$ is evaluated approaching the real axis from above. Equation (10) can be immediately derived from the analytic continuation of $K^{(2)}(z)$ for $z < 0$, which can be obtained from Eq. (6) replacing $y(z)$, for $z > 0$, with $1/y(z)$, for $z < 0$.

If in Eq. (9) one uses the explicit expression for $\mathrm{Im}K^{(2)}(t/m^2)$ of Eq. (10) and changes the integration variable from t to $x = 1+y$ via the substitution

$$t(x) = \frac{m^2 x^2}{x-1}, \tag{12}$$

obtained from Eq. (5), one finds [28]

$$a_\mu^{\mathrm{HVP}}(\mathrm{LO}) = \frac{\alpha}{\pi}\int_0^1 \mathrm{d}x\, \kappa^{(2)}(x)\, \Delta\alpha_{\mathrm{h}}(t(x)), \tag{13}$$

where the space-like kernel is remarkably simple,

$$\kappa^{(2)}(x) = 1 - x \tag{14}$$

and $\Delta\alpha_{\mathrm{h}}(t) = -\Pi_{\mathrm{h}}(t)$ is the (five-flavor) hadronic contribution to the running of the effective fine-structure constant in the space-like region.

Equation (13) (or forms equivalent to it) is used in lattice QCD calculations of $a_\mu^{\mathrm{HVP}}(\mathrm{LO})$ (see e.g. [29] and a discussion in [7]). It also forms the basis for the MUonE proposal to determine $a_\mu^{\mathrm{HVP}}(\mathrm{LO})$ via muon-electron scattering data [20–23].

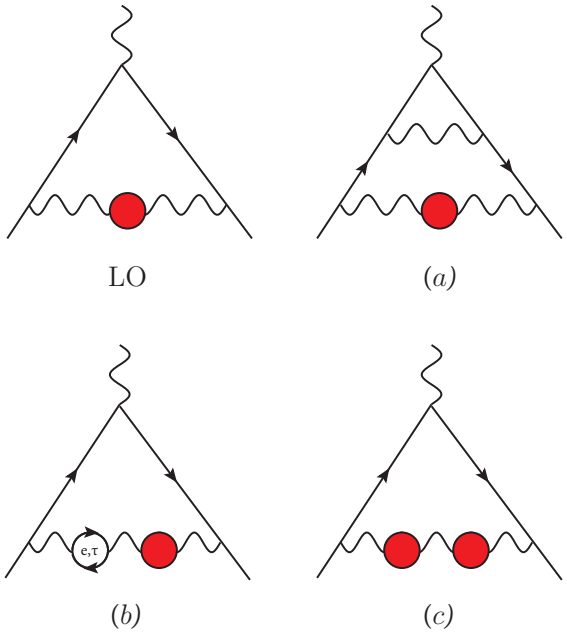

Figure 1: LO and sample NLO diagrams contributing to the HVP contribution to the muon g-2.

3. The HVP contribution at NLO

The hadronic vacuum polarization contribution to the muon g-2 at next-to-leading order, $a_\mu^{\mathrm{HVP}}(\mathrm{NLO})$, is due to three classes of diagrams of order $\mathcal{O}(\alpha^3)$, see Fig. 1. Class (a) consists of diagrams with one single HVP insertion in one of the photon lines of the two-loop QED diagrams contributing to the muon g-2, without any vacuum polarization insertion due to electron or tau loops. Class (b) contains diagrams with one HVP and one additional vacuum polarization due to an electron or tau loop. Finally, class (c) consists of the diagram with two HVPs. Numerically, class (a) yields the largest (negative) contribution, class (b) partially cancels it, and the contribution of class (c) is very small, as expected. These contributions will be called $a_\mu^{(a)}$, $a_\mu^{(b)}$ and $a_\mu^{(c)}$, respectively, with

$$a_\mu^{\mathrm{HVP}}(\mathrm{NLO}) = a_\mu^{(a)} + a_\mu^{(b)} + a_\mu^{(c)}. \tag{15}$$

3.1. Class (a)

The NLO HVP contribution of class (a) to the muon g-2 can be written in the time-like form [27]

$$a_\mu^{(a)} = \frac{\alpha^2}{\pi^3}\int_{s_0}^\infty \frac{\mathrm{d}s}{s}\, 2K^{(4)}(s/m^2)\, \mathrm{Im}\Pi_{\mathrm{h}}(s). \tag{16}$$

The fourth-order function $K^{(4)}(z)$ was first computed by Barbieri and Remiddi in [27].[1] Its lengthy expression is reported in their Eq. (3.21) for $z > 0$, where it is real and negative. An approximate series expansion for $K^{(4)}(s/m^2)$ in the parameter m^2/s, with terms up to fourth order, can be found in [30].

Like $K^{(2)}(z)$, the function $K^{(4)}(z)$ is real for any $z \geq 0$, has a cut for $z < 0$, and satisfies the dispersion relation

$$K^{(4)}(z) = \frac{1}{\pi}\int_{-\infty}^0 \mathrm{d}z'\, \frac{\mathrm{Im}K^{(4)}(z')}{z'-z}, \quad z > 0. \tag{17}$$

Just as we did for $a_\mu^{\mathrm{HVP}}(\mathrm{LO})$, using the dispersion relations (8) and (17) the NLO hadronic contribution of class (a) can be cast in the space-like form

$$a_\mu^{(a)} = -\frac{\alpha^2}{\pi^3}\int_{-\infty}^0 \frac{\mathrm{d}t}{t}\, \Pi_{\mathrm{h}}(t)\, 2\mathrm{Im}K^{(4)}(t/m^2). \tag{18}$$

To compute $\mathrm{Im}K^{(4)}(t/m^2)$, first we analytically continue the $K^{(4)}(z)$ expression of Ref. [27] from $z > 0$ to $z < 0$, replacing $y(z)$ with $1/y(z)$ in order

[1] Note the coefficient 2 in front of the function $K^{(4)}(z)$ due to the original normalization chosen in Ref. [27].

to choose coherently the Riemann sheets on the cut. Then, taking the imaginary parts of the resulting polylogarithms (of order 1, 2, and 3), we obtain[2]

$$\mathrm{Im}K^{(4)}(z+i\epsilon) = \pi\,\theta(-z)\,F^{(4)}(y(z)), \qquad (19)$$

where

$$\begin{aligned} F^{(4)}(y) &= R_1(y) + R_2(y)\ln(-y) \\ &\quad + R_3(y)\ln(1+y) + R_4(y)\ln(1-y) \\ &\quad + R_5(y)\big[4\mathrm{Li}_2(y) + 2\mathrm{Li}_2(-y) \\ &\qquad + \ln(-y)\ln\big((1-y)^2(1+y)\big)\big], \end{aligned} \qquad (20)$$

and the rational functions $R_i(y)$ $(i = 1, \ldots, 5)$ are

$$\begin{aligned} R_1 &= \frac{23y^6 - 37y^5 + 124y^4 - 86y^3 - 57y^2 + 99y + 78}{72(y-1)^2 y(y+1)}, \\ R_2 &= \frac{12y^8 - 11y^7 - 78y^6 + 21y^5 + 4y^4 - 15y^3 + 13y + 6}{12(y-1)^3 y(y+1)^2}, \\ R_3 &= \frac{(y+1)\left(-y^3 + 7y^2 + 8y + 6\right)}{12y^2}, \\ R_4 &= \frac{-7y^4 - 8y^3 + 8y + 7}{12y^2}, \\ R_5 &= -\frac{3y^4 + 5y^3 + 7y^2 + 5y + 3}{6y^2}. \end{aligned} \qquad (21)$$

The dilogarithm is $\mathrm{Li}_2(y) = -\int_0^y (\mathrm{d}u/u)\ln(1-u)$.

Using the explicit expression for $\mathrm{Im}K^{(4)}(t/m^2)$ of Eq. (19), Eq. (18) can be conveniently expressed in terms of the variable $x = 1 + y$. We obtain

$$a_\mu^{(a)} = \left(\frac{\alpha}{\pi}\right)^2 \int_0^1 \mathrm{d}x\,\kappa^{(4)}(x)\,\Delta\alpha_{\rm h}(t(x)), \qquad (22)$$

where

$$\kappa^{(4)}(x) = \frac{2-x}{x\,(x-1)}\,2F^{(4)}(x-1). \qquad (23)$$

For $0 \le x < 1$, $z \le 0$. Equation (22) is the analogue of Eq. (13) for the NLO contribution of class (a). Figure 2 shows the space-like functions $\kappa^{(2)}(x)$ and $\kappa^{(4)}(x)$ entering the $a_\mu^{\rm HVP}(\mathrm{LO})$ and $a_\mu^{(a)}$ expressions, respectively. We note that the function $\kappa^{(4)}(x)$ provides a stronger weight to $\Delta\alpha_{\rm h}(q^2)$ at large negative values of q^2 than $\kappa^{(2)}(x)$. In particular, for $q^2 \to -\infty$, $\kappa^{(2)}(1) = 0$, whereas

[2]After presenting our $\mathrm{Im}K^{(4)}(z)$ result, Eqs.(19–21), in [31] (see also [32]), we were informed by Alexander Nesterenko that he has independently derived it in [33].

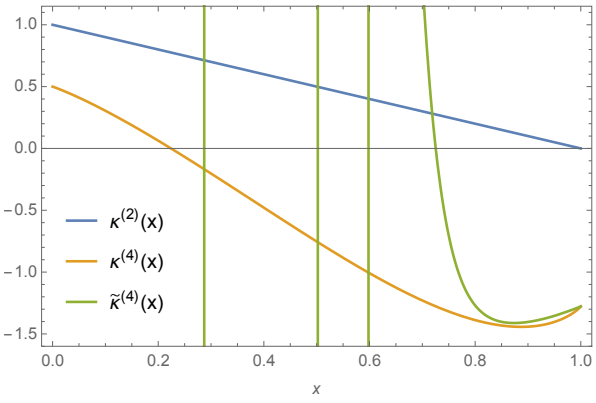

Figure 2: The space-like functions $\kappa^{(2)}(x)$ (blue), $\kappa^{(4)}(x)$ (orange) and $\tilde{\kappa}^{(4)}(x)$ (green).

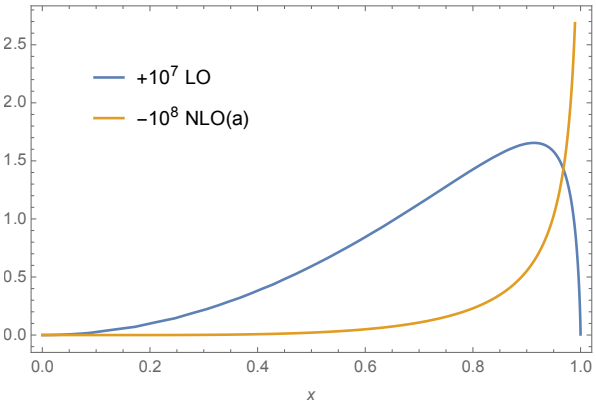

Figure 3: The integrands $(\alpha/\pi)\kappa^{(2)}(x)\Delta\alpha_{\rm h}(t(x))$ (blue) and $(\alpha/\pi)^2\kappa^{(4)}(x)\Delta\alpha_{\rm h}(t(x))$ (orange) of Eqs.(13) and (22), multiplied by 10^7 and -10^8, respectively.

$\kappa^{(4)}(1) = -23/18$. Figure 3 shows the LO integrand $(\alpha/\pi)\kappa^{(2)}(x)\Delta\alpha_{\rm h}(t(x))$ of Eq. (13) and the NLO integrand $(\alpha/\pi)^2\kappa^{(4)}(x)\Delta\alpha_{\rm h}(t(x))$ of Eq. (22), multiplied by 10^7 and -10^8, respectively. The LO integrand has a peak at $x \sim 0.914$, where $t \sim -(0.33\mathrm{GeV})^2$. On the other hand, the NLO integrand of class (a) increases monotonically with $x \to 1$ (i.e. with $t \to -\infty$) like $\sim \ln(1-x)$.

An approximate expression for the space-like formula in Eq. (22) was provided in Ref. [34]. To obtain it, the authors started considering the approximate fourth-order series expansion of Ref. [30] for the time-like function $K^{(4)}(s/m^2)$ in the small parameter $r = m^2/s$. This series expansion only contains powers r^n of degree $n = 1, 2, 3, 4$, multiplied by constants, $\ln r$, and $(\ln r)^2$ terms. Then,

as suggested in [35], they exploited generating integral representations to fit the r^n and $r^n \ln r$ terms of the approximate fourth-order series expansion for $K^{(4)}(1/r)$, but not the $r^n(\ln r)^2$ ones, and used the usual dispersion relation satisfied by $\Pi_{\rm h}(q^2)$ to perform the integral over s. After some simple changes of variables, their approximation can be compared with our exact function $\kappa^{(4)}(x)$. We repeated the analysis of Ref. [34] confirming their approximate result (in particular, their Eqs. (A1,A2)) which, translated in our notation, will be called here $\tilde{\kappa}^{(4)}(x)$.

The approximate function $\tilde{\kappa}^{(4)}(x)$ is plotted in Fig. 2 (indicated by the green line). While the exact function $\kappa^{(4)}(x)$ varies smoothly over the entire region $0 \le x \le 1$, $\tilde{\kappa}^{(4)}(x)$ strongly oscillates, leading to large numerical cancelations when employed in the integral of Eq. (22) instead of $\kappa^{(4)}(x)$. Using the Fortran libraries KNT18VP [36–41] for the numerical implementation of $\Delta\alpha_{\rm h}(t(x))$ in the space-like region, we computed two numerical values for $a_\mu^{(a)}$ in Eq. (22): one obtained using the exact function $\kappa^{(4)}(x)$ and a second one obtained replacing $\kappa^{(4)}(x)$ with the approximate $\tilde{\kappa}^{(4)}(x)$. The two values differ by about 3%. Adding to $a_\mu^{(a)}$ the contributions $a_\mu^{(b)}$ and $a_\mu^{(c)}$ (discussed later), the total $a_\mu^{\rm HVP}({\rm NLO})$ contribution computed using the $\tilde{\kappa}^{(4)}(x)$ approximation differs from the one computed via our exact function $\kappa^{(4)}(x)$ by about 6%.

It is interesting to investigate the source of the above $\sim 6\%$ discrepancy. To improve the $\tilde{\kappa}^{(4)}(x)$ approximation, we proceeded in two directions. The first one consisted in repeating the analysis of Ref. [34], starting however from higher-order series expansions for the exact $K^{(4)}(s/m^2)$ function of Barbieri and Remiddi [27] (we considered n up to $n_{\rm max} = 24$), rather than from the fourth-order (i.e. $n_{\rm max} = 4$) series expansion for $K^{(4)}(s/m^2)$ of Ref. [30]. Our second improvement consisted in exploiting generating integral representations to fit the r^n, $r^n \ln r$, as well as the $r^n(\ln r)^2$ terms which were omitted in the analysis of Ref. [34]. Our studies show that the inclusion of the $r^n(\ln r)^2$ terms greatly improves the $\kappa^{(4)}(x)$ approximations, even if the order $n_{\rm max}$ of the series expansion for $K^{(4)}(s/m^2)$ is not increased above four. Calling $\bar{\kappa}^{(4)}(x, n_{\rm max})$ our improved approximation for $\kappa^{(4)}(x)$ obtained including $r^n(\ln r)^2$ terms starting from the series expansion for $K^{(4)}(s/m^2)$ up to order $n_{\rm max}$, we verified that the total $a_\mu^{\rm HVP}({\rm NLO})$ contribution computed using our $\bar{\kappa}^{(4)}(x, 4)$ differs by less than one per mille from the one computed via our exact function $\kappa^{(4)}(x)$. Even better agreements were reached increasing the order $n_{\rm max}$.

The authors of Ref. [34] added an $O(10\%)$ uncertainty to their final result to take into account the error induced by the omission of the $r^n(\ln r)^2$ terms. This uncertainty, which dominates the error of their final result, can be eliminated using the simple formula for $\kappa^{(4)}(x)$ provided in this paper.

3.2. Classes (b) and (c)

The space-like expressions for the class (b) and (c) NLO HVP contributions to the muon g-2 are [34]

$$a_\mu^{(b)} = \frac{\alpha}{\pi} \int_0^1 {\rm d}x\, \kappa^{(2)}(x)\, \Delta\alpha_{\rm h}(t(x)) \times 2 \left[\Delta\alpha_e^{(2)}(t(x)) + \Delta\alpha_\tau^{(2)}(t(x)) \right], \quad (24)$$

$$a_\mu^{(c)} = \frac{\alpha}{\pi} \int_0^1 {\rm d}x\, \kappa^{(2)}(x)\, \left[\Delta\alpha_{\rm h}(t(x))\right]^2, \quad (25)$$

where $\Pi_\ell^{(2)}(t) = -\Delta\alpha_\ell^{(2)}(t)$ is the renormalized one-loop QED vacuum polarization function in the space-like region, with a lepton $\ell = e, \tau$ in the loop,

$$\Pi_\ell^{(2)}(t) = \frac{\alpha}{\pi} \left[\frac{8}{9} - \frac{\beta_\ell^2}{3} + \beta_\ell \left(\frac{1}{2} - \frac{\beta_\ell^2}{6} \right) \ln \frac{\beta_\ell - 1}{\beta_\ell + 1} \right] \quad (26)$$

and $\beta_\ell = \sqrt{1 - 4m_\ell^2/t}$. Equations (24,25) can be immediately obtained from the time-like formulae of Ref. [30] using the usual dispersion relation satisfied by $\Pi_{\rm h}(t)$ and $\Pi_\ell^{(2)}(t)$ to perform the integrals over s [28, 34].

Figure 4 shows the NLO integrands of Eqs. (22), (24), and (25), multiplied by -10^8, 10^8, and 10^8, respectively.

4. Conclusions

In this paper we provided simple exact analytic expressions to extend the computation of the hadronic vacuum polarization contribution to the muon g-2 in the space-like region up to next-to-leading order. These results can be employed to determine very precisely $a_\mu^{\rm HVP}({\rm NLO})$, which is due to three classes of diagrams of order $\mathcal{O}(\alpha^3)$, via lattice QCD as well as scattering data like those expected of the proposed MUonE experiment at CERN. In fact, it would be very interesting to compute precisely, besides $a_\mu^{\rm HVP}({\rm LO})$, also the $a_\mu^{\rm HVP}({\rm NLO})$ term

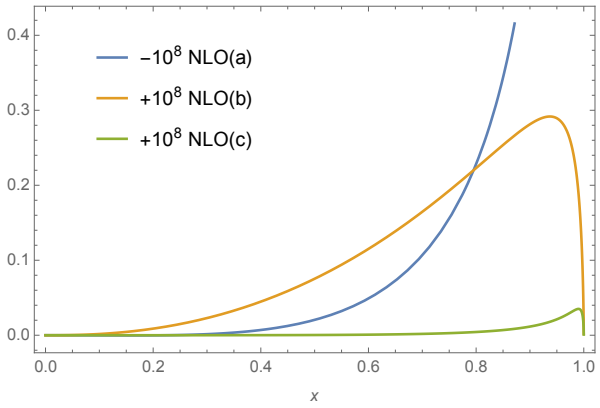

Figure 4: The NLO integrands of Eqs. (22) (blue), (24) (orange), and (25) (green), multiplied by -10^8, 10^8, and 10^8, respectively.

on the lattice. This would provide consistent and precise NLO comparisons of the HVP contribution to the muon g-2 computed via lattice QCD with results already obtained via time-like data.

Existing approximations for the NLO function $\kappa^{(4)}(x)$ induced the largest source of uncertainty in the NLO lattice QCD calculation of Ref. [34]. This uncertainty, of $O(10\%)$, can be eliminated using the exact expression for $\kappa^{(4)}(x)$ provided in this paper.

Finally, the NLO weight functions of the $a_\mu^{\rm HVP}$(NLO) contributions were found to differ significantly from the LO one of $a_\mu^{\rm HVP}$(LO). In particular, the function $\kappa^{(4)}(x)$ provides a stronger weight to $\Delta\alpha_{\rm h}(q^2)$ at large negative values of q^2 than $\kappa^{(2)}(x)$. These different weights may help shed light on the tension between the lattice BMW determination of the LO HVP contribution to the muon g-2 and those obtained with time-like data.

Acknowledgments We would like to thank A. Keshavarzi and W. J. Marciano for useful discussions and correspondence. We are also grateful to all our MUonE colleagues for our stimulating collaboration. M. P. acknowledges partial support from the EU Horizon 2020 research and innovation programme under the Marie Sklodowska-Curie grant agreements 690575 (RISE InvisiblesPlus) and 674896 (ITN ELUSIVES). This project has received funding/support from the EU Horizon 2020 research and innovation programme under the Marie Sklodowska-Curie grant agreement No 860881-HIDDEN.

References

[1] B. Abi, et al. (Muon g-2), Phys. Rev. Lett. 126 (2021) 141801. doi:10.1103/PhysRevLett.126.141801. arXiv:2104.03281.

[2] T. Albahri, et al. (Muon g-2), Phys. Rev. D 103 (2021) 072002. doi:10.1103/PhysRevD.103.072002. arXiv:2104.03247.

[3] T. Albahri, et al. (Muon g-2), Phys. Rev. A 103 (2021) 042208. doi:10.1103/PhysRevA.103.042208. arXiv:2104.03201.

[4] T. Albahri, et al. (Muon g-2), Phys. Rev. Accel. Beams 24 (2021) 044002. doi:10.1103/PhysRevAccelBeams.24.044002. arXiv:2104.03240.

[5] G. W. Bennett, et al. (Muon g-2), Phys. Rev. D 73 (2006) 072003. doi:10.1103/PhysRevD.73.072003. arXiv:hep-ex/0602035.

[6] M. Abe, et al., PTEP 2019 (2019) 053C02. doi:10.1093/ptep/ptz030. arXiv:1901.03047.

[7] T. Aoyama, et al., Phys. Rept. 887 (2020) 1–166. doi:10.1016/j.physrep.2020.07.006. arXiv:2006.04822.

[8] F. Jegerlehner, The Anomalous Magnetic Moment of the Muon, volume 274, Springer, Cham, 2017. doi:10.1007/978-3-319-63577-4.

[9] G. Colangelo, M. Hoferichter, P. Stoffer, JHEP 02 (2019) 006. doi:10.1007/JHEP02(2019)006. arXiv:1810.00007.

[10] M. Hoferichter, B.-L. Hoid, B. Kubis, JHEP 08 (2019) 137. doi:10.1007/JHEP08(2019)137. arXiv:1907.01556.

[11] M. Davier, A. Hoecker, B. Malaescu, Z. Zhang, Eur. Phys. J. C 80 (2020) 241. doi:10.1140/epjc/s10052-020-7792-2. arXiv:1908.00921, [Erratum: Eur.Phys.J.C 80, 410 (2020)].

[12] A. Keshavarzi, D. Nomura, T. Teubner, Phys. Rev. D 101 (2020) 014029. doi:10.1103/PhysRevD.101.014029. arXiv:1911.00367.

[13] A. Kurz, T. Liu, P. Marquard, M. Steinhauser, Phys. Lett. B 734 (2014) 144–147. doi:10.1016/j.physletb.2014.05.043. arXiv:1403.6400.

[14] S. Borsanyi, et al., Nature 593 (2021) 51–55. doi:10.1038/s41586-021-03418-1. arXiv:2002.12347.

[15] M. Passera, W. J. Marciano, A. Sirlin, Phys. Rev. D 78 (2008) 013009. doi:10.1103/PhysRevD.78.013009. arXiv:0804.1142.

[16] A. Keshavarzi, W. J. Marciano, M. Passera, A. Sirlin, Phys. Rev. D 102 (2020) 033002. doi:10.1103/PhysRevD.102.033002. arXiv:2006.12666.

[17] A. Crivellin, M. Hoferichter, C. A. Manzari, M. Montull, Phys. Rev. Lett. 125 (2020) 091801. doi:10.1103/PhysRevLett.125.091801. arXiv:2003.04886.

[18] B. Malaescu, M. Schott, Eur. Phys. J. C 81 (2021) 46. doi:10.1140/epjc/s10052-021-08848-9. arXiv:2008.08107.

[19] G. Colangelo, M. Hoferichter, P. Stoffer, Phys. Lett. B 814 (2021) 136073. doi:10.1016/j.physletb.2021.136073. arXiv:2010.07943.

[20] C. M. Carloni Calame, M. Passera, L. Trentadue, G. Venanzoni, Phys. Lett. B 746 (2015) 325–329. doi:10.1016/j.physletb.2015.05.020. arXiv:1504.02228.

[21] G. Abbiendi, et al., Eur. Phys. J. C 77 (2017) 139. doi:10.1140/epjc/s10052-017-4633-z. arXiv:1609.08987.

[22] G. Abbiendi, et al., Letter of Intent: The MUonE Project, CERN-SPSC-2019-026 / SPSC-

I-252, 2019. http://cds.cern.ch/record/2677471/files/SPSC-I-252.pdf?version=1.
[23] P. Banerjee, et al., Eur. Phys. J. C 80 (2020) 591. doi:10.1140/epjc/s10052-020-8138-9. arXiv:2004.13663.
[24] C. Bouchiat, L. Michel, J. Phys. Radium 22 (1961) 121–121. doi:10.1051/jphysrad:01961002202012101.
[25] S. J. Brodsky, E. De Rafael, Phys. Rev. 168 (1968) 1620–1622. doi:10.1103/PhysRev.168.1620.
[26] B. E. Lautrup, E. De Rafael, Phys. Rev. 174 (1968) 1835–1842. doi:10.1103/PhysRev.174.1835.
[27] R. Barbieri, E. Remiddi, Nucl. Phys. B 90 (1975) 233–266. doi:10.1016/0550-3213(75)90645-8.
[28] B. e. Lautrup, A. Peterman, E. de Rafael, Phys. Rept. 3 (1972) 193–259. doi:10.1016/0370-1573(72)90011-7.
[29] T. Blum, Phys. Rev. Lett. 91 (2003) 052001. doi:10.1103/PhysRevLett.91.052001. arXiv:hep-lat/0212018.
[30] B. Krause, Phys. Lett. B 390 (1997) 392–400. doi:10.1016/S0370-2693(96)01346-9. arXiv:hep-ph/9607259.
[31] S. Laporta, Talk given at the STRONG 2020 Virtual Workshop on "Spacelike and Timelike determination of the Hadronic Leading Order contribution to the Muon g-2", November 26, 2021. https://agenda.infn.it/event/28089.
[32] M. Passera, Talk given at "Inspired by Precision", Symposium in honor of Professor Ettore Remiddi's 80th birthday, Accademia delle Scienze, Bologna, Italy, December 10, 2021. https://agenda.infn.it/event/28554.
[33] A. V. Nesterenko (2021). arXiv:2112.05009.
[34] B. Chakraborty, C. T. H. Davies, J. Koponen, G. P. Lepage, R. S. Van de Water, Phys. Rev. D 98 (2018) 094503. doi:10.1103/PhysRevD.98.094503. arXiv:1806.08190.
[35] S. Groote, J. G. Korner, A. A. Pivovarov, Eur. Phys. J. C 24 (2002) 393–405. doi:10.1007/s10052-002-0958-2. arXiv:hep-ph/0111206.
[36] R. V. Harlander, M. Steinhauser, Comput. Phys. Commun. 153 (2003) 244–274. doi:10.1016/S0010-4655(03)00204-2. arXiv:hep-ph/0212294.
[37] K. Hagiwara, A. D. Martin, D. Nomura, T. Teubner, Phys. Rev. D 69 (2004) 093003. doi:10.1103/PhysRevD.69.093003. arXiv:hep-ph/0312250.
[38] K. Hagiwara, A. D. Martin, D. Nomura, T. Teubner, Phys. Lett. B 649 (2007) 173–179. doi:10.1016/j.physletb.2007.04.012. arXiv:hep-ph/0611102.
[39] S. Actis, et al. (Working Group on Radiative Corrections, Monte Carlo Generators for Low Energies), Eur. Phys. J. C 66 (2010) 585–686. doi:10.1140/epjc/s10052-010-1251-4. arXiv:0912.0749.
[40] K. Hagiwara, R. Liao, A. D. Martin, D. Nomura, T. Teubner, J. Phys. G 38 (2011) 085003. doi:10.1088/0954-3899/38/8/085003. arXiv:1105.3149.
[41] A. Keshavarzi, D. Nomura, T. Teubner, Phys. Rev. D 97 (2018) 114025. doi:10.1103/PhysRevD.97.114025. arXiv:1802.02995.